ELECTROPHORETIC IMMOBILIZATION OF TIO_2 PHOTOCATALYST ON AL, CU, CU/NI AND PET PLATES FOR PHOTODEGRADATION OF PHENOL

by

LIM CHOO KEAN

June 2004

Thesis submitted in fulfillment of the requirements for the degree of Doctor of Philosophy

ACKNOWLEDGEMENTS

I would like to express my gratitude to my dedicated main supervisor, Assoc. Prof. Mohd. Asri Mohd. Nawi for all the guidance and advice to me throughout my candidature. I have learned a great deal in the field of photocatalysis because of the unlimited knowledge being poured by him to me. I would also like to thank Dr. Md. Sariff Jab. who is my co-supervisor and Assoc. Prof. Jamil Ismail who is the dean of school of chemical sciences. My special thanks also go out to Prof. Keiichi Tanaka from Oita University, Japan who has collaborated with our research. Special thanks also go out to the Ministry of Science, Technology and Environment for granting me a Special Scholarship during my candidature. Beside that, I would like to thank the staff of the School of Chemical Sciences and Institute of Postgraduate Studies, USM for the assistance provided.

Last but not least, I would like to thank my family and my wife for their understanding, never-ending moral support and patience during my candidature.

TABLE OF CONTENTS

Contents Page Number

Title i

Acknowledgement ii

Table of Contents iii

List of Tables ix

List of Figures x

Abstrak xvi

Abstract xviii

CHAPTER 1: Introduction 1

1.1 General 1

1.2 Photocatalysts 2

  1.2.1 Titanium Dioxide 3

  1.2.2 Application of TiO_2 Photocatalysis 4

1.3 Heterogeneous TiO_2 Photocatalysis 6

  1.3.1 Activation 8

  1.3.2 Effect of Various Factors 14

    1.3.2.1 Mass of Catalyst 14

    1.3.2.2 Wavelength 16

    1.3.2.3 Initial Concentration 16

    1.3.2.4 Temperature 17

    1.3.2.5 Radiant Flux 18

  1.3.3 Preparation and Modification 20

1.3.4 Inorganics and Metal Ions Remediation 21

1.3.5 Activity Evaluation 21

1.3.5.1 Kinetic 22

1.3.6 Immobilized Photocatalysts 24

1.4 Treatment of Phenol 28

1.4.1 Mechanistic Studies 29

1.4.2 pH 33

1.4.3 Inorganic Ions 35

1.4.4 Added Oxidant 37

1.5 Statement of Problems 39

1.6 The Research Objectives 39

CHAPTER 2: Experimental 41

2.1 Materials 41

2.2 Immobilization of TiO_2 Photocatalyst onto Support Substrates 42

2.3 Determination of Photocatalytic Efficiency of Immobilized TiO_2 Photocatalyst 43

2.3.1 Analysis of Phenol 46

2.3.2 Determination of Photocatalytic Activity 46

2.3.3 SEM Micrographs 47

2.3.4 Analysis of Metal Ions 47

2.4 Aluminium Base as Support Material 47

2.4.1 Optimization of Electrophoretic Deposition 48

2.4.1.1 Effect of Potential 48

2.4.1.2 Effect of Concentration of TiO_2 Suspension 48

2.4.2 Effect of ENR on Deposition of TiO_2 49

2.4.2.1 Study of TiO_2 Deposition 49

2.4.2.2 Determination of Settling of TiO_2 Suspension 50

2.4.2.3 Strength of TiO_2 Deposit Layer 50

2.4.2.4 Determination of Optimum ENR Doped TiO_2 Suspension Solution for Electrophoretic Deposition 51

2.4.3 Determination of Optimum Deposit of TiO_2-ENR Photocatalyst 51

2.4.4 Comparison of Photocatalytic Activity of Various TiO_2 Immobilized Plates 52

2.4.5 Reproducibility Studies of Thermal Treatment on Immobilized TiO_2 and TiO_2-ENR Plates 52

2.4.6 Morphology Study of Al/TiO_2 and Al/ENRTiO_2 Plates 53

2.4.7 Deactivation Study of Al/TiO_2 by Different Al Species 53

2.4.8 Attempts to Identify Products of Phenol Degradation by Immobilized TiO_2 Plates with HPLC 53

2.4.9 Comparison of Photocatalytic Efficiency of Immobilized TiO_2 with Suspension Mode and Sol-Gel Method 54

2.4.9.1 Suspension Mode 54

2.4.9.2 Sol-Gel Method 54

2.4.9.3 Analysis of Total Organic Carbon 55

2.5 Copper, Copper/Nickel Bimetal, Silver Coated Polyethylene Terephthalate (PET/Ag) and Graphite Coated Polyethylene Terephthalate (PET/C) Plates as Support Material 56

2.5.1 Determination of Optimum Deposit on Copper, Copper/Nickel, PET/silver and PET/carbon Plates 56

2.5.2 Study of Plate's Reproducibility 56

2.5.3 Study of Metal Ions Leached 57

2.5.4 Comparison of Final Products of Phenol Degradation 57

2.5.5 Optimization of Solution Parameters for Photocatalysis with Cu/Ni/ENRTiO_2 Plate 58

2.5.5.1 Effect of pH, H_2O_2 and Total Organic Carbon 58

2.5.6 Effect of Anions and Cations on the Photocatalytic Activities of Cu/Ni/ENRTiO_2, PET/Ag/ENRTiO_2 and PET/C/ENRTiO_2 Plate 59

CHAPTER 3: Results and Discussion: Aluminium Plates as Support Material **61**

3.1 Optimization of Electrophoretic Deposition 61

3.2 Effect of ENR on Deposition of TiO_2 63

3.3 Determination of Optimum Deposit of TiO_2-ENR Photocatalyst 73

3.4 Comparison of Photocatalytic Activities of Various TiO_2 Immobilized Plates 78

3.5 Reproducibility Studies of Thermal Treatment on Immobilized TiO_2 Plates 78

3.6 Deactivation Study of Al/TiO_2 by Different Al Species 84

3.7 Attempts to Identify Products of Phenol Degradation by Immobilized TiO_2 Plates 87

3.8 Comparison of Photocatalytic Efficiency of Immobilized TiO_2 with Suspension Mode and Sol-Gel Method 93

3.9 Conclusions 100

CHAPTER 4: Results and Discussion: Copper and Copper/Nickel Bimetal Plates as Support Material 103

4.1 Determination of Optimum Deposit on Copper and Copper/Nickel Plates 104

4.2 Study of Plate’s Reproducibility 104

4.3 Study of Metal Ions Leached 107

4.4 Comparison of Final Products of Phenol Degradation 112

4.5 Optimization of Solution Parameters for Photocatalysis with Cu/Ni/ENRTiO$_2$ Plates 117

  4.5.1 Effect of pH 117

  4.5.2 Effect of H_2O_2 120

4.6 Effect of Anions and Cations on the Photocatalytic Activities of Cu/Ni/ENRTiO$_2$ Plate 123

4.7 Conclusions 131

CHAPTER 5: Results and Discussion: PET/Silver and PET/Carbon Plates as Support Material 133

5.1 Determination of Optimum Deposit on PET/silver and PET/carbon Plates 133

5.2 Study of Plate’s Reproducibility 135

5.3 Comparison of Final Products of Phenol Degradation 137

5.4 Effect of Anions and Cations on the Photocatalytic Activities of PET/Ag/ENRTiO$_2$ and PET/C/ENRTiO$_2$ Plates 141

5.5 Conclusions 145

CHAPTER 6: Final Remarks **146**

References **150**

Appendices:

Appendix A: Seminars, conferences or symposiums participated during candidature 163

A.1 Abstract: Immobilized TiO_2 Photocatalyst on Metal Support for the Degradation of Phenol. 165

A.2 Abstract: Phenol Degradation by Immobilized TiO_2 Photocatalyst. Part 1: TiO_2 Immobilized onto Al Plate. 167

A.3 Abstract: Photocatalytic Degradation of Phenol by Immobilized Photocatalyst. Part 2: TiO_2 Immobilized onto Cu Plate. 168

A.4 Abstract: Photocatalytic Degradation of Phenol by Immobilized Photocatalyst. Part 3: TiO_2 Immobilized onto Cu/Ni Plate. 169

Appendix B: Publications 170

B.1 Lim Choo Kean, Keiichi Tanaka, Shariff Jab and Mohd. Asri Nawi (2002). “Photocatalytic Degradation of Phenol by Immobilized Photocatalyst. Part 2: TiO_2 Immobilized onto Cu Plate.” *Malaysian J. Chem.*, **4(1)**, 60-64. 171

B.2 Lim Choo Kean, Keiichi Tanaka, Shariff Jab and Mohd. Asri Nawi (2002). “Photocatalytic Degradation of Phenol by Immobilized Photocatalyst. Part 3: TiO_2 Immobilized onto Cu/Ni Plate.” *Malaysian J. Chem.,* **4(1)**, 65-70. 176

B.3 Mohd. Asri Nawi, Lim Choo Kean, Keiichi Tanaka, Md. Shariff Jab (2003). “Fabrication of Photocatalytic TiO_2-Epoxidized Natural Rubber on Al Plate via Electrophoretic Deposition.” *Appl. Catal. B: Environ.*, **46**, 165-174. 182

Appendix C: Calculation and preparation 192

Appendix D: Data 198

List of Tables

Tables		Page Number
Table 1.1	General reaction scheme of TiO_2 photocatalysis.	12
Table 4.1	$t_{½}$ and TOC of the photocatalytic degradation of 20 mL 0.10 mM phenol solution by H_2O_2, Cu/Ni/ENRTiO_2 and Cu/Ni/ENRTiO_2 + H_2O_2 and suspension.	122
Table 4.2	$t_{½}$ of photocatalytic degradation of 20 mL 0.10 mM phenol solution by Cu/Ni/ENRTiO_2, in the presence of various anions. All anions were prepared by sodium salt with the anion concentration of 0.10 M.	124
Table 4.3	$t_{½}$ of photocatalytic degradation of 20 mL 0.10 mM phenol solution by epoxy polymer coated Cu/Ni/ENRTiO_2, in the presence of various anions. All anions were prepared by sodium salt with the anion concentration of 0.10 M.	126
Table 4.4	$t_{½}$ of photocatalytic degradation of 20 mL 0.10 mM phenol solution by Cu/Ni/ENRTiO_2, in the presence of various cations. All cations were prepared by chloride and/or sulphate salt with the concentration showed in Appendix C.5.	128
Table 5.1	$t_{½}$ of photocatalytic degradation of 20 mL 0.10 mM phenol solution by PET/Ag/ENRTiO_2, in the presence of various anions. All anions were prepared by sodium salt with the anion concentration of 0.10 M.	142
Table 5.2	$t_{½}$ of photocatalytic degradation of 20 mL 0.10 mM phenol solution by PET/Ag/ENRTiO_2, in the presence of various cations. All cations were prepared by chloride and/or sulphate salt with the concentration showed in Appendix C.5.	142
Table 5.3	$t_{½}$ of photocatalytic degradation of 20 mL 0.10 mM phenol solution by PET/C/ENRTiO_2, in the presence of various anions. All anions were prepared by sodium salt with the anion concentration of 0.10 M.	144
Table 5.4	$t_{½}$ of photocatalytic degradation of 20 mL 0.10 mM phenol solution by PET/C/ENRTiO_2, in the presence of various cations. All cations were prepared by chloride and/or sulphate salt with the concentration showed in Appendix C.5	144

List of Figures

Figures		Page Number
Figure 1.1	Illustration of the major process occurring on a TiO_2 particle following electronic excitation. Electron-hole recombination can occur at the surface (reaction (a)) or in the bulk (reaction (b)) of the TiO_2. At the surface of the particle, photogenerated electrons can reduce an electron acceptor A (reaction (c)) and photogenerated holes can oxidize an electron donor D (reaction (d)). The combination of reactions (c) and (d) represents the TiO_2 sensitization of the general redox reaction.	9
Figure 1.2	Illustration of the heterogeneous TiO_2 photocatalysis process. Excitation of TiO_2 particle generating electro-hole pairs that in turn generate hydroxyl radical either from dissolved oxygen or water molecules. Two hydroxyl radicals generated per photon of light.	11
Figure 1.3	Influence of the different physical parameters that govern the reaction rate (generally comprised between 0.1 – 1 mM): (a) mass of catalyst; (b) wavelength; (c) initial concentration of reactant; (d) temperature and (e) radiant flux.	15
Figure1.4	Proposed mechanism of photocatalytic degradation of phenol.	31
Figure 2.1	Schematic diagram for the preparation of immobilized TiO_2.	44
Figure 2.2	Schematic diagram of the photocatalytic degradation of phenol solution by immobilized TiO_2.	45
Figure 3.1	$t_{½}$ of photocatalytic degradation of 20 mL 0.10 mM phenol solution by Al/TiO_2 and weight of deposit, as a function of deposition potential.	62
Figure 3.2	$t_{½}$ of photocatalytic degradation of 20 mL 0.10 mM phenol solution by Al/TiO_2, as a function of concentration of TiO_2 suspension.	64
Figure 3.3	Weight of TiO_2 deposit, as a function of time during the deposition of TiO_2 onto Al plates. Al/ENRTiO_2 was prepared in the presence of 0.50 g ENR in 250 mL TiO_2 suspension. Deposition potential was 110 V. Amount of TiO_2 was 2.50 g in 250 mL acetone.	66

Figure 3.4 Settling volume versus time of TiO_2 suspension with and without the presence of ENR in 50 mL measuring cylinder. 67

Figure 3.5 % TiO_2 retained on Al plates as a function of time of sonication. Al/ENRTiO_2 was prepared in the presence of 0.50 g ENR in 250 mL TiO_2 suspension. The initial deposit was 1.0 mg / cm^2. 69

Figure 3.6 % TiO_2 retained on Al plates after 10 second sonication versus weight of ENR solution added into the 250 mL suspension for the immobilization. The initial deposit was 1.0 mg / cm^2. 70

Figure 3.7 $t_{½}$ value of the photocatalytic degradation of 20 mL 0.10 mM phenol solution by Al base immobilized TiO_2, as a function of weight of ENR solution added into the 250 mL suspension. Deposition potential was 110 V and the deposit on all plates was 1.0 mg / cm^2. The $t_{½}$ of 12.74 minutes represents Al/TiO_2 for comparison. 72

Figure 3.8 Rate constant (*k*) versus TiO_2 deposit for Al plate immobilized TiO_2 with and without the presence of ENR on the photocatalytic degradation of 20 mL 0.10 mM phenol solution. Al/ENRTiO_2 was prepared in the presence of 0.50 g ENR in 250 mL TiO_2 suspension. The time of photocatalytic degradation was fixed for 2 hours. 74

Figure 3.9 SEM micrographs of (a) Al/TiO_2 and (b) Al/ENRTiO_2 at 1,000 X magnification and Al/ENRTiO_2 with (c) 0.5 (d) 1.0 (e) 1.5 and (f) 2.0 mg / cm^2 deposit at 10,000 X magnification. Scale bar for (a) and (b) was 20.0 μm whereas for (c), (d), (e) and (f) was 2.00 μm.Al/ENRTiO_2 was prepared as Al/TiO_2 except with the addition of 0.50 g ENR into 250 mL suspension. 75

Figure 3.10 Particle size and coverage, as a function of TiO_2 deposited on Al/ENRTiO_2. 77

Figure 3.11 Photocatalytic degradation of 20 mL 0.10 mM phenol solution as a function of time, comprising two immobilized TiO_2 plates, with and without ENR, photolysis alone, immobilized rutile TiO_2 and a blank consisted of bare Al plates. Al/ENRTiO_2 was prepared in the presence of 0.50 g ENR in 250 mL TiO_2 suspension. The deposit on the Al plates was 1.0 mg / cm^2. 79

Figure 3.12 $t_{½}$ of photocatalytic degradation of 20 mL 0.10 mM phenol solution by Al/TiO_2 at different thermal treatment temperature, as a function of repetition. 81

Figure 3.13 $t_{½}$ of photocatalytic degradation of 20 mL 0.10 mM phenol solution by Al/ENRTiO_2 at different thermal treatment temperature, as a function of repetition. 83

Figure 3.14 Particle size and coverage, as a function of thermal treatment temperature for 1 hour of Al/TiO_2 and Al/ENRTiO_2. 85

Figure 3.15 Photocatalytic degradation of 20 mL 0.20 mM phenol solution by Al/TiO_2 in the presence of 10 mM $Al(OH)_3$, Al_2O_3, HCl and NaOH. 86

Figure 3.16 (a) Typical HPLC chromatogram of photocatalytic degradation of 20 mL 0.10 mM phenol solution by Al/TiO_2. The time given in the x-axis (in min.) represent the time duration of photocatalytic degradation of phenol solution by the Al/TiO_2 plate. Retention time (in min.) for each peak is shown on the chromatogram itself. 88

Figure 3.16 (b) Typical HPLC chromatogram of photocatalytic degradation of 20 mL 0.10 mM phenol solution by Al/ENRTiO_2. The time given in the x-axis (in min.) represent the time duration of photocatalytic degradation of phenol solution by the Al/ENRTiO_2 plate. Retention time (in min.) for each peak is shown on the chromatogram itself. 89

Figure 3.17 % peak area of major intermediates during the photocatalytic degradation of 20 mL 0.10 mM phenol solution by Al/TiO_2, as a function of time. 91

Figure 3.18 % peak area of major intermediates during the photocatalytic degradation of 20 mL 0.10 mM phenol solution by Al/ENRTiO_2, as a function of time. 92

Figure 3.19 Photocatalytic degradation of 20 mL 0.10 mM phenol solution at different concentrations of TiO_2 suspension. 94

Figure 3.20 Typical HPLC chromatogram of photocatalytic degradation of 20 mL 0.10 mM phenol solution by 1 g/L TiO_2 suspension. The time given in the x-axis (in min.) represent the time duration of photocatalytic degradation of phenol solution by the suspension. Retention time (in min.) for each peak is shown on the 95 chromatogram itself.

Figure 3.21 $t_{½}$ of photocatalytic degradation of 20 mL 0.10 mM phenol solution by sol-gel prepared Al/TiO_2 (SG) and Glass/TiO_2 (SG). 96

Figure 3.22 (a) Typical HPLC chromatogram of photocatalytic degradation of 20 mL 0.10 mM phenol solution by Al/TiO_2 prepared by sol-gel method. The time given in the x-axis (in min.) represent the time duration of photocatalytic degradation of phenol solution by the Al/TiO_2 plate. Retention time (in min.) for each peak is shown on the chromatogram itself. 98

Figure 3.22 (b) Typical HPLC chromatogram of photocatalytic degradation of 20 mL 0.10 mM phenol solution by Glass/TiO_2 prepared by sol-gel method. The time given in the x-axis (in min.) represent the time duration of photocatalytic degradation of phenol solution by the Glass/TiO_2 plate. Retention time (in min.) for each peak is shown on the chromatogram itself. 99

Figure 3.23 Total organic carbon (TOC) of photocatalytic degradation of 20 mL 0.10 mM phenol solution by Al/TiO_2, Al/ENRTiO_2, Al/TiO_2 (SG), Al/Rutile and suspension, as a function time. 101

Figure 4.1 Rate constant (*k*) versus TiO_2 deposit for Cu/ENRTiO_2 and Cu/Ni/ENRTiO_2 on the photocatalytic degradation of 20 mL 0.10 mM phenol solution. The immobilized TiO_2 was prepared in the presence of 0.50 g ENR in 250 mL TiO_2 suspension. 105

Figure 4.2 $t_{½}$ of photocatalytic degradation of 20 mL 0.10 mM phenol solution by Cu/ENRTiO_2 and Cu/Ni/ENRTiO_2, as a function of repetition. 106

Figure 4.3 Cumulative Cu^{2+} ions leaching for Cu/ENRTiO_2 on the degradation of 20 mL 0.10 mM phenol solution upon reuse. 108

Figure 4.4 Metal ions leached for Cu/Ni/ENRTiO_2 on the degradation of 20 mL 0.10 mM phenol upon reuse. 110

Figure 4.5 Photos of (a) Cu/ENRTiO_2 and (b) Cu/Ni/ENRTiO_2, before and after photocatalytic degradation of 20 mL 0.10 mM phenol solution. The white surface is the TiO_2 layer and the brown spot represents the deposition of copper on the TiO_2 surface. The 111 dimension of the plate was 4.5 cm X 5.5 cm. Magnification: ~ 0.81X.

Figure 4.6 (a) Typical HPLC chromatogram of photocatalytic degradation of 20 mL 0.10 mM phenol solution by Cu/ENRTiO_2. The time given in the x-axis (in min.) represent the time duration of photocatalytic degradation of phenol solution by the Cu/ENRTiO_2 plate. Retention time (in min.) for each peak is shown on the chromatogram itself. 113

Figure 4.6 (b) Typical HPLC chromatogram of photocatalytic degradation of 20 mL 0.10 mM phenol solution by Cu/Ni/ENRTiO_2. The time given in the x-axis (in min.) represent the time duration of photocatalytic degradation of phenol solution by the Cu/Ni/ENRTiO_2 plate. Retention time (in min.) for each peak is shown on the chromatogram itself. 114

Figure 4.7 % peak area of major intermediates during the photocatalytic degradation of 20 mL 0.10 mM phenol solution by Cu/ENRTiO_2, as a function of time. 115

Figure 4.8 % peak area of major intermediates during the photocatalytic degradation of 20 mL 0.10 mM phenol solution by Cu/Ni/ENRTiO_2, as a function of time. 116

Figure 4.9 $t_{½}$ of photocatalytic degradation of 20 mL 0.10 mM phenol solution by Cu/Ni/ENRTiO_2, as a function of pH. The Cu^{2+} and Ni^{2+} ions leached during the phenol degradation at respective pH were presented in the table. 118

Figure 4.10 $t_{½}$ of photocatalytic degradation of 20 mL 0.10 mM phenol solution by Cu/Ni/ENRTiO_2, as a function of concentration of H_2O_2. The Cu^{2+} and Ni^{2+} ions leached during the phenol degradation at Cu/Ni/ENRTiO_2 with 5.0 mM and 10.0 mM H_2O_2 were presented in the table. 121

Figure 4.11 Effect of epoxy polymer coated Cu/Ni/ENRTiO_2 on metal ion leaching on 20 mL 0.10 phenol degradation with various anions interferences. B and A indicates Cu/Ni/ENRTiO_2 before and after the coating of epoxy polymer, respectively. All anions were prepared by sodium salt with the anion concentration of 0.10 M. 125

Figure 4.12 Concentration of metal ions leached versus cations prepared from its chloride salt. 129

Figure 4.13 Concentration of metal ions leached versus cations prepared from its sulphate salt. 130

Figure 5.1 Rate constant (*k*) versus TiO_2 deposit for PET/Ag/ENRTiO_2 and PET/C/ENRTiO_2 on the photocatalytic degradation of 20 mL 0.10 mM phenol solution. The immobilized TiO_2 was prepared in the presence of 0.50 g ENR in 250 mL TiO_2 suspension. 134

Figure 5.2 $t_{½}$ of photocatalytic degradation of 20 mL 0.10 mM phenol solution by PET/Ag/ENRTiO_2 and PET/C/ENRTiO_2, as a function of repetition. The concentration of Ag^+ ions leached from PET/Ag/ENRTiO_2 was provided. 136

Figure 5.3 Typical HPLC chromatogram of photocatalytic degradation of 20 mL 0.10 mM phenol solution by (a) PET/Ag/ENRTiO_2 and (b) PET/C/ENRTiO_2. The multiple peaks showing the changes in concentration of phenol and intermediates as a function of irradiation time for the irradiation time 0 to 90 min.. 138

Figure 5.4 % peak area of major intermediates during the photocatalytic degradation of 20 mL 0.10 mM phenol solution by PET/Ag/ENRTiO_2, as a function of time. 139

Figure 5.5 % peak area of major intermediates during the photocatalytic degradation of 20 mL 0.10 mM phenol solution by PET/C/ENRTiO_2, as a function of time. 140

PEMEGUNAN ELEKTROFORETIK FOTOMANGKIN TIO_2 PADA PLAT-PLAT AL, CU, CU/NI DAN PET UNTUK FOTOPENGURAIAN FENOL

ABSTRAK

Fotomangkin terpegun Al/TiO_2, Al/ENRTiO_2, Cu/ENRTiO_2, Cu/Ni/ENRTiO_2, PET/Ag/ENRTiO_2 dan PET/C/ENRTiO_2 disediakan dengan kaedah pengenapan elektroforetik terubahsuai. Keaktifan fotomangkin dikaji dengan penguraian 20 mL 0.10 mM larutan fenol. Kadar pemegunan dan kekuatan lapisan endapan dipertingkatkan dengan penambahan ENR (epoxidized natural rubber). Masa separuh hayat, $t_{½,,}$ dalam minit didapati mengikuti urutan PET/C/ENRTiO_2 (5.92) < PET/Ag/ENRTiO_2 (7.27) < Cu/Ni/ENRTiO_2 (10.7) < Al/TiO_2 (12.74) < Cu/ENRTiO_2 (13.0) < Al/ENRTiO_2 (18.38). Semua TiO_2 terpegun memberikan keaktifan fotomangkin yang semakin meningkat apabila diulangi, kecuali dengan penyokong substrat Al. Walaupun keaktifan fotomangkin dengan penyokong Al meningkat dengan peningkatan suhu perawatan, keaktifan fotomangkin didapati menurun apabila diulangi. Ion-ion Cu^{2+} dan Ni^{2+} didapati melucut daripada permukaan Cu dan Cu/Ni semasa fotopenguraian. Nilai maksimum larut lesap ialah 0.48 ppm Cu^{2+} bagi Cu/ENRTiO_2 dan 0.09 ppm Cu^{2+} dan 0.09 ppm Ni^{2+} bagi Cu/Ni/ENRTiO_2. Walau bagaimanapun, kelarutlesapan ion-ion logam didapati berkurangan apabila proses perawatan diulangi dan akhirnya memenuhi keperluan had pembuangan DOE iaitu 1.00 ppm. Kelarutlesapan Ag^+ daripada PET/Ag/ENRTiO_2 yang dianggap kesan gangguan ion-ion boleh diabaikan kesan kehadirannya. Nitrat, klorida, sulfat, hidrogen karbonat, dihidrogen fosfat dan fosfat ke atas penguraian penol juga telah dikaji. Penguraian fenol oleh Cu/Ni/ENRTiO_2 didapati meningkat dengan kehadiran nitrat. Pembantutan kuat oleh fosfat dalam penguraian fenol dengan Cu/Ni/ENRTiO$_2$ dan PET/Ag/ENRTiO$_2$ didapati tidak berlaku dengan ketara untuk sistem PET/C/ENRTiO$_2$. Kesan gangguan kation-kation yang dikaji ialah K^+, Na^+, Ca^{2+}, Mg^{2+}, Zn^{2+}, Ni^{2+}, Cu^{2+}, Fe^{2+}, Al^{3+} dan Cr^{3+} yang disediakan daripada garam klorida dan/atau sulfat. Hanya Cr^{3+} memberikan kesan negatif daripada semua kation yang dikaji. Keaktifan fotomangkin yang disediakan dengan kaedah elektroforetik adalah setanding dari segi masa penguraian total dengan mod ampaian dan lebih tinggi berbanding dengan kaedah sol-gel. Total mineralisasi fenol boleh dicapai masing-masing sehingga 91.12, 78.64 dan 65.68 % dengan Cu/Ni/ENRTiO$_2$, Al/TiO$_2$ dan Al/ENRTiO$_2$. Penguraian fenol dengan fotomangkin terpegun mempunyai pelbagai laluan tindak balas, bergantung kepada jenis penyokong substrat dan keadaan-keadaan operasi.

ABSTRACT

Immobilized photocatalysts referred to as Al/TiO_2, Al/ENRTiO_2, Cu/ENRTiO_2, Cu/Ni/ENRTiO_2, PET/Ag/ENRTiO_2 and PET/C/ENRTiO_2 were prepared by modified electrophoretic deposition method. The photocatalytic activity of these immobilized TiO_2 was evaluated by degradation of 20 mL 0.10 mM phenol in aqueous solution. The rate of immobilization and the strength of deposited layer were enhanced by the addition of ENR (epoxidized natural rubber). Under the optimised conditions, the $t_{½}$ in minutes of phenol degradation follow the sequence of PET/C/ENRTiO_2 (5.92) < PET/Ag/ENRTiO_2 (7.27) < Cu/Ni/ENRTiO_2 (10.7) < Al/TiO_2 (12.74) < Cu/ENRTiO_2 (13.0) < Al/ENRTiO_2 (18.38). Except for Al plate, all immobilized TiO_2 plates gave improved and sustained photocatalytic activity upon reuse. The photocatalytic activity of Al supported photocatalyst increased with an increase in calcined temperature, but with the drawback of reduced photocatalytic activity upon reused. Cu^{2+} and Ni^{2+} ions were leached from the surface of Cu and Cu/Ni supports during the photodegradation. The maximum value of metal ions leached were 0.48 ppm Cu^{2+} ion for Cu/ENRTiO_2 and 0.09 ppm Cu^{2+} ion and 0.09 ppm Ni^{2+} ion for Cu/Ni/ENRTiO_2. However, the metal ions leached decreased upon reuse and passed the discharge limit of DOE requirement of 1.00 ppm. The Ag^+ ion leach-out from PET/Ag/ENRTiO_2 was negligible. Interferences from anions such as nitrate, chloride, sulphate, hydrogen carbonate, dihydrogen phosphate and phosphate of sodium salt were studied. In the presence of nitrate, the degradation of phenol by Cu/Ni/ENRTiO_2 was significantly improved. The strong inhibition by phosphate in the degradation of phenol by Cu/Ni/ENRTiO_2 and PET/Ag/ENRTiO_2 plates however did not occur when PET/C/ENRTiO_2 was used instead. The effect of interferences from cations such as K^+, Na^+, Ca^{2+}, Mg^{2+}, Zn^{2+}, Ni^{2+}, Cu^{2+}, Fe^{2+}, Al^{3+} and Cr^{3+} were studied and each cation was prepared from either its chloride and/or sulphate salts. Only Cr^{3+} ion was found to give negative interference effect. The photocatalytic activity of immobilized TiO_2 prepared by electrophoretic method was comparable in terms of total degradation time with suspension mode but higher than sol-gel method. Total mineralization of phenol can be achieved up to 91.12, 78.64 and 65.68 % by Cu/Ni/ENRTiO_2, Al/TiO_2 and Al/ENRTiO_2, respectively. Immobilized photocatalysis of phenol have different reaction pathways, depending on the support substrates and conditions.

1 Introduction

1.1 General

The toxic waste disposal of household and industrial effluents has become a problem of growing importance in modern society. In recent years, research on new methods for water purification has moved from processes involving phase transfer towards processes concerning the chemical destruction of the contaminants such as advanced oxidation process (AOP). Heterogeneous photocatalysis has engrossed much attention for its highly effective photocatalytic function of treating a variety of contaminants in the environment (Hoffmann *et al.*, 1995). Its main attraction is the ability to produce complete mineralization of pollutants including those persistent organic without addition of chemicals to the treated water. By utilization of titanium dioxide photocatalyst, many different chemicals, including those that are resistant to normal oxidation reactions, have been proven to be detoxified, removed or mineralized (Ollis *et al.*, 1991; Tinucci *et al.*, 1992; Ray, 1998). The complete mineralization of organics makes this area as one of the fore front of current research in the treatment of water and air pollution.

Photocatalysis can be defined as the acceleration of a photoreaction (light-induced transformation of chemical species) by the presence of a catalyst (Mills and Hunte, 1997). A more in depth approach would comprise that the catalyst may accelerate the photoreaction by interaction with the substrate in its ground or excited state and/or with a primary photoproduct, depending upon the mechanism of the photoreaction (Kutal and Serpone, 1993).

There are more than 6200 citations and 2355 patents of works published between 1970 and the middle of 2001, in using heterogeneous photocatalytic oxidation of organic or inorganic compounds in air or water and on the photocatalytic reduction of inorganic compounds in water (Blake, 2001). The photocatalytic oxidation of organic compounds in water has received the most interest (Tinucci *et al.*, 1993; Matthews, 1986; Okamoto *et al.*, 1985). The most-studied compounds are phenol derivatives, dye compounds, pesticides and herbicides (Chiron *et al.*, 1999; Matthews, 1993).

1.2 Photocatalysts

Wide bandgap semiconductor such as oxides (TiO_2, ZnO, WO_3 and Fe_2O_3) and chalcogenides (commonly CdS) was commonly employed as photocatalyst in heterogeneous photocatalysis (Kamat, 1993). Titanium dioxide in the anatase form appears to be the most photoactive and the most practical of the semiconductors for widespread environmental applications such as water purification, wastewater treatment, hazardous waste control, air purification, and water disinfection (Fujishima *et al.*, 2000). ZnO appears to be a suitable alternative to TiO_2, but it is unstable with respect to incongruous dissolution to yield $Zn(OH)_2$ on the ZnO particle surface, thus leading to catalyst inactivation over time. Metal sulfide and iron oxide polymorphs are not suitable photocatalyst because they readily undergo photoanodic and photocathodic corrosion respectively.

1.2.1 Titanium dioxide

Titanium dioxide, TiO_2, is an ore deposit obtained from either ilmenite (titanium iron rocks, $TiFeO_3$, containing 45-65% TiO_2) or rutile beach sand. It is polymorphous solid, exists in three modifications or crystal structures, which are anatase, rutile and brookite. Rutile is the more common and more well known mineral of the three, while anatase is the rarest. Anatase is thermodynamically less stable than rutile, but its formation is kinetically favored at temperature below 600 ^{o}C (Herrmann, 1999). Only the anatase and rutile modifications are of any note, technically or commercially.

TiO_2 production is achieved through one of two methods, which are referred to as the sulfate process and the chloride process. Sulphuric acid is used in the sulphate route (SR) to attack the titanium feedstock and on the other hand, chlorine gas is used in the chloride route (CR) (Oh, S.-M and Park, D.-W., 2001). The chloride process is taking over as the preferred procedure. In the year 2000 approximately 60% of world production of TiO_2 is by the chloride process.

The most important function of titanium dioxide is as a white pigment for providing brightness, whiteness and opacity to products such as paints and coatings, plastics, paper, inks, fibers, ceramics and food and cosmetics. However, another important emerging use is as photocatalyst in the breakdown of toxic organics and precipitation of heavy metals from water and wastewater. The most effective modification for this purpose is the anatase crystal structure.

1.2.2 Application of TiO_2 photocatalysis

The application of TiO_2 as photocatalyst can be classified into amenity (anti-staining, non-fogging, antibacterial and deodorizing), environment purification (air and water purification), and energy development technologies (production of H_2, solar cells and reduction of CO_2) (Fujishima *et al.*, 2000, Nukui, 2000).

A combination of a TiO_2 photocatalyst and a hydrophilic silicone material, when exposed to UV light, forms a thin layer of water, which is called a super-hydrophilic phenomenon. This may be used to prevent adhesion of water drops on material surfaces, to prevent fogging of glass, or provide self-cleaning effect by which dust is washed off easily by rainfall or sprayed water. Non-fogging drop-free side mirrors for vehicles and automotive body coat that retains non-staining performance are products that utilize the super-hydrophilic property of catalysts (Hata *et al.*, 2000).

The public awareness over the spread of pathogenic bacterial and germs infection is increasing and needs for sterilization and antibacterial measures. When used as an antibacterial agent in the present of light, a TiO_2 photocatalyst not only has a strong ability as a disinfectant but also decomposes and removes the dead germs and even toxins. A study showed that TiO_2 oxidation effectively removed Escheria coli (E. coli) from drinking water (Sökmen *et al.*, 2001).

Deodorization can be achieved by masking (with aromatic agents), adsorption (with active carbons), neutralization (with chemicals), oxidation (with ozone, catalysts, etc.), or biological process (microorganisms). Photocatalytic deodorizing falls under the oxidation category, which is more ideal than others in terms of deodorizing capacity, safety, durability, and cost. This type of photocatalysts is used in such commercial products such as air purifiers, air conditioners, and deodorizing fibers (Pichat *et al.*, 2000).

Photocatalysts can decompose most organic or inorganic substances in air or water by photocatalytic oxidation and reduce harmful inorganic substances in water. This technology has been used to detoxify drinking water, decontaminate industrial wastewater, and purify air streams. For example, catalysts are drawing much attention as the means of air purification especially for the treatment of CO, CO_2, NOx, SOx and VOCs emission from automobiles, which presents a serious concern of the health hazards (Nukui, 2000).

Water pollutant removal by TiO_2 photocatalytic detoxification appears as the most promising potential application since many toxic water pollutants, either organic or inorganic, are totally mineralized or oxidized at their higher degree, respectively, into harmless final compounds (Hoffmann *et al.*, 1995). The process is efficient, economically feasible and environmental friendly. In recent years, the success of laboratory work has led to interest in applying the technology to environmental remediation and process waste stream treatment. Numerous papers have addressed topics relevant to designing reactors or kinetic modeling for photocatalytic processes such as non-concentrating reactor (Feitz *et al.*, 2000; Gimenez *et al.*, 1999), compound parabolic concentrator (Fernandez-Ibanez *et al.*, 1999; Gimenez *et al.*, 1999; Marques *et al.*, 1997; Curco *et al.*, 1996), flat plate reactor (Augugliaro *et al.*, 1995), controlled periodic illumination and light scattering model.

Many studies have been made regarding the use of photocatalysts such as in the production of H_2, fixation of CO_2, and artificial photosynthesis. But they are yet far from realization due to the low reactive efficiency. Other areas of study include electrochemical solar cells based on TiO_2 photocatalysts. Electrochemical solar cells are formed by using a TiO_2 photocatalyst as an electrode and placing an inactive electrode (example Pt) in the other side of the electrolyte to form a circuit (Phani *et al.*, 2001).

1.3 Heterogeneous TiO_2 Photocatalysis

Photocatalysis process provides several ‘green’ characteristics. Among these are:

a. The safe anatase TiO_2,
b. Molecular oxygen as oxidant,
c. Work under ambient conditions,
d. Clean and no sludge produced, and
e. A general mechanistic oxidation toward various contaminant classes involving hydroxyl radicals.

In heterogeneous photocatalysis, TiO_2 is illuminated with near-UV light, promoting an electron from the valence band to the conduction band, generating electron-hole pairs that in turn generate hydroxyl radicals. The latter degrade a large number of organic compounds to carbon dioxide, water and mineral acids (Hisanaga *et al.*, 1990; Dillert *et al.*, 1999). The chemical oxidant is generated *in situ* from dissolved oxygen or water, therefore provides a mechanism for sustainable usage of photocatalyst.

The nature of the TiO_2 determines the rate and efficiency of the process. TiO_2 in anatase form is believed to be the most efficient photocatalysts for heterogeneous photocatalysis (Heung and Anderson, 1996). The anatase form of TiO_2 has the desirable properties of being:

a. chemically inert,
b. photostable,
c. photoactive,
d. cheap,
e. readily available,
f. non-toxic, and
g. high oxidative power as a catalyst for oxidation processes (Fujishima and Rao, 1997, Fujishima *et al.*, 2000).

Additionally, TiO_2 can be coated as a thin film on a support and can be activated by sunlight (Alberici and Jardim, 1994). The wide 3.2 eV energy band gap matches the output of a wide variety of readily available lamps but is not ideal for solar applications although it is able to utilize visible and/or near-UV light. Rutile form of TiO_2 has a smaller band gap, 3.0 eV, but only a few reports observe photocatalytic activity for this form (Sclafani *et al.*, 1990).

1.3.1 Activation

The mechanism of photocatalytic destruction of hazardous organic compounds on UV-irradiated TiO_2 in aerated water is widely known and well-examined in TiO_2 suspensions (Al-Sayyed *et al.*, 1991; Kamat, 1993; Hoffmann *et al.*, 1995). This anatase-assisted oxidation process takes place at the surface of TiO_2 substrate and the photoexcited TiO_2 then transfer an electron into a ground state molecule (Linsebigler *et al.*, 1995).

Figure 1.1 demonstrates the electronic excitation process occurring on a TiO_2 particle. When a TiO_2 (anatase) semiconductor is illuminated with photons whose energy is equal to or greater than their band-gap energy E_G ($\lambda < 385$ nm), there is absorption of these photons and creation within the bulk of electron-hole pairs, which dissociate (charge separation) into free photoelectrons in the conduction band and photoholes in the valence band (Herrmann, 1995; 1999). The energy level at the bottom of the conduction band reflects the reduction potential of the photoelectron, whereas the upper-most level of the valence band is a measure of the oxidizing ability of the photohole. Hence reductive and oxidative processes for adsorbed couples with redox potentials more positive and more negative than the different energy of the conduction and valence band, respectively, can be driven by surface-trapped e^- and h^+ carriers (Serpone, 1997).

Simultaneously, in the presence of an aqueous phase, a spontaneous adsorption occurs and according to the redox potential (or energy level) of each adsorbate, an electron transfer proceeds towards acceptor molecules, whereas positive

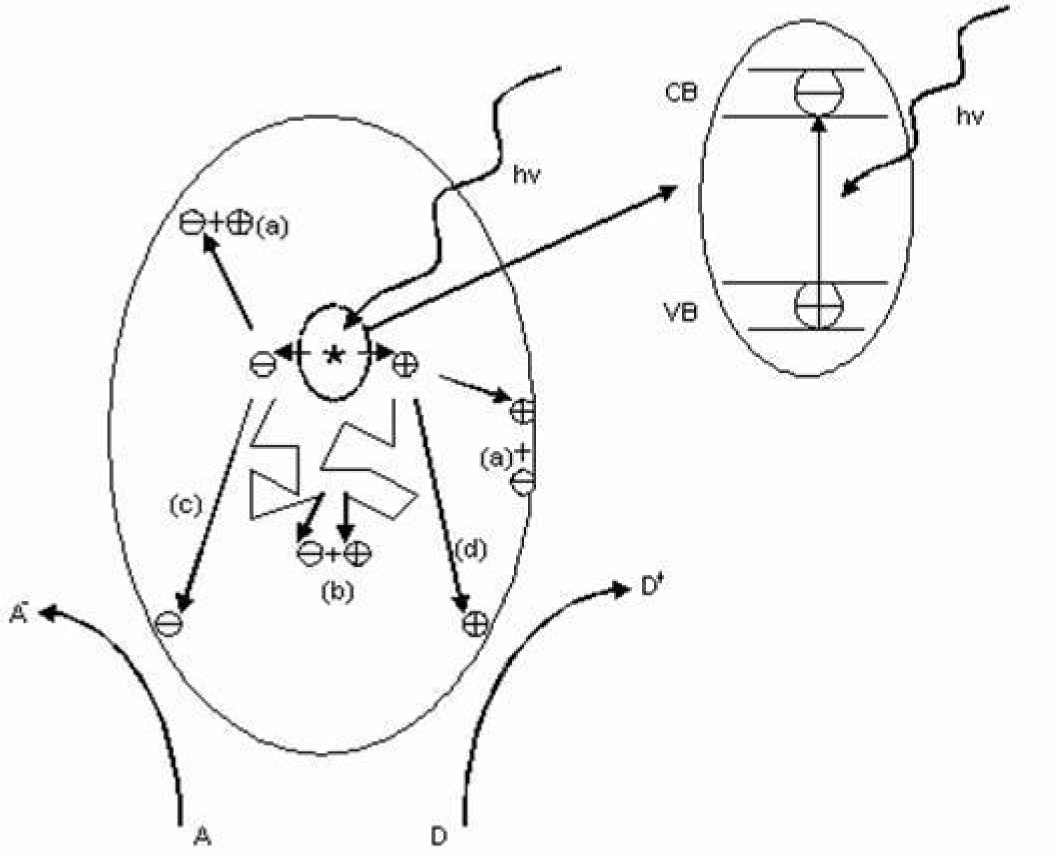

Figure 1.1 Illustration of the major process occurring on a TiO_2 particle following electronic excitation. Electron-hole recombination can occur at the surface (Reaction (a)) or in the bulk (Reaction (b)) of the TiO_2. At the surface of the particle, photogenerated electrons can reduce an electron acceptor A (Reaction (c)) and photogenerated holes can oxidize an electron donor D (Reaction (d)). The combination of Reactions (c) and (d) represents the TiO_2 sensitization of the general redox reaction (Ollis and Al-Ekabi, 1993; Hoffmann *et al.*, 1995; Mills and Hunte, 1997).

photohole are transferred to donor molecules (actually the hole transfer corresponds to the cession of an electron by the donor to the solid) as shows in Figure 1.2 (Herrmann, 1995; 1999).

Hydroxyl radicals, $OH^\bullet$, are formed by the reaction of free or trapped holes at the semiconductor surface with adsorbed water or hydroxide ions (Vidal, 1998). The photogenerated electron is usually considered to be trapped at the surface where it is then irreversibly scavenged by a suitable electron acceptor, most usually oxygen (Mills and Wang, 1999; Mills and Hunte, 1997; Hoffmann *et al.*, 1995; Ku *et al.*, 1996). As a result, surface O_2^- is formed; this ion can be reduced further to H_2O_2, $OH^\bullet$, and OH^-. The produced species may react with the organic radicals formed in the oxidative route (Fujishima *et al.*, 2000). Therefore, the organic compounds present in the illuminated TiO_2 slurry undergo many chain, consecutive, and other reactions (Herrmann, 1995; 1999; Ollis and Al-Ekabi, 1993; Serpone and Schiavello, 1988). Finally, in an ideal case, all intermediate compounds are fully mineralized, i.e. they are oxidized to CO_2 and H_2O (Sobezynski *et al.*, 1999).

A reaction sequence proposed by Turchi and Ollis (1990) is shown in Table 1.1 and includes the following steps:

(a) catalyst activation by radiation,
(b) adsorption of water, the organic compound and the generated hydroxyl radical on the catalytic surface,
(c) recombination of electrons and holes,
(d) hole trapping by the adsorbed species,
(e) electron trapping, having oxygen as the main electron acceptor,

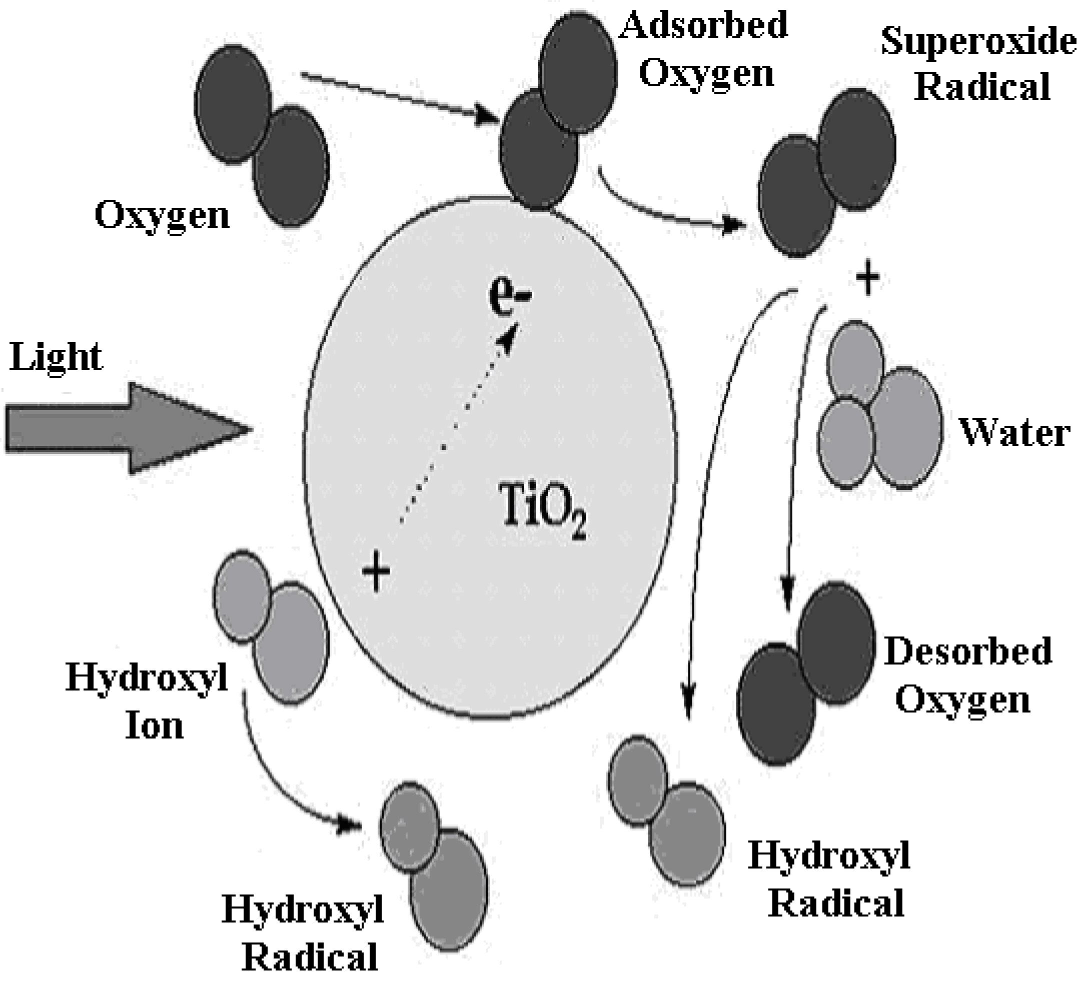
Adsorbed Oxygen
Superoxide Radical
Oxygen
e-
Light
+
Water
TiO2
+
Hydroxyl Ion
Desorbed Oxygen
Hydroxyl Radical
Hydroxyl Radical

Figure 1.2 Illustration of the heterogeneous TiO_2 photocatalysis process. Excitation of TiO_2 particle generating electro-hole pairs that in turn generate hydroxyl radical either from dissolved oxygen or water molecules. Two hydroxyl radicals generated per photon of light (Hisanaga *et al.*, 1990; Dillert *et al.*, 1999).

(a) Activation $\mathrm{TiO_2} \xrightarrow{hv} \mathrm{e^- + h^+}$ (1.1)

(b) Adsorption

$\mathrm{O^{2-} + Ti^{IV} + H_2O \leftrightarrow OH^- + Ti^{IV} - OH^-}$ (1.2)

$\mathrm{Ti^{IV} + H_2O \leftrightarrow Ti^{IV} - H_2O}$ (1.3)

$\mathrm{site} + \mathrm{R}_i \leftrightarrow \mathrm{R}_{i,\mathrm{ads}}$ (1.4)

$\mathrm{OH^\bullet + Ti^{IV} \leftrightarrow Ti^{IV} \,|\, OH^\bullet}$ (1.5)

(c) Recombination

$\mathrm{e^- + h^+ \rightarrow heat}$ (1.6)

(d) Hole trapping

$\mathrm{Ti^{IV} - OH^- + h^+ \leftrightarrow Ti^{IV} \,|\, OH^\bullet}$ (1.7)

$\mathrm{Ti^{IV} - H_2O + h^+ \leftrightarrow Ti^{IV} \,|\, OH^\bullet + H^+}$ (1.8)

$\mathrm{R}_{i,\mathrm{ads}} + \mathrm{h^+} \leftrightarrow \mathrm{R}^{+}_{i,\mathrm{ads}}$ (1.9)

(e) Electron trapping

$\mathrm{Ti^{IV} + e^- \leftrightarrow Ti^{III}}$ (1.10)

$\mathrm{Ti^{III} + O_2 \leftrightarrow Ti^{IV} + O_2^-}$ (1.11)

(f) Hydroxyl attach

Case I $\mathrm{Ti^{IV} \,|\, OH^\bullet} + \mathrm{R}_{i,\mathrm{ads}} \rightarrow \mathrm{Ti^{IV}} + \mathrm{R}_{j,\mathrm{ads}}$ (1.12)

Case II $\mathrm{OH^\bullet} + \mathrm{R}_{i,\mathrm{ads}} \rightarrow \mathrm{R}_{j,\mathrm{ads}}$ (1.13)

Case III $\mathrm{Ti^{IV} \,|\, OH^\bullet} + \mathrm{R}_i \rightarrow \mathrm{Ti^{IV}} + \mathrm{R}_j$ (1.14)

Case IV $\mathrm{OH^\bullet} + \mathrm{R}_i \rightarrow \mathrm{R}_j$ (1.15)

Table 1.1 General reaction scheme of $\mathrm{TiO_2}$ photocatalysis (Turchi and Ollis, 1990; Gerischer, 1993).

(f) $OH^{\bullet}$ radical attack on the substrate R_i, and reaction of the $OH^{\bullet}$ radical with different compounds [Rj (j=1, 2,…, n; $j \neq i$], including reaction products or intermediates.

The photocatalytic efficiency can be reduced by the electron-hole recombination, which corresponds to the degradation of the photoelectric energy into heat. Therefore, the key issue governing the efficiency of photocatalytic oxidative degradation is minimizing electron-hole recombination by maximizing the rate of interfacial electron transfers to trap the photogenerated electron and/or hole (Hoffmann *et al.*, 1995; 1999).

Okamoto *et al.* (1985) proposed the formation of hydroxyl-free radicals resulted from the UV-excitation of TiO_2 to produce holes for reaction with water or OH^-, and also from a series of chain reactions of oxygen molecules to form H_2O_2 and then $OH^{\bullet}$. If the pK_a (4.88) of the $OH^{\bullet}$ is lower than the pH of solution, the decrease of $HO_2^{\bullet}$ concentration will not promote subsequent chain reactions of H_2O_2 formation. Turchi and Ollis (1989) and Matthews (1986) also proposed that UV-excited TiO_2 formed electron/hole pairs. The holes react with water or OH^- to form $OH^{\bullet}$ or directly oxidize organic matters, while the electrons react with oxygen to form peroxy-free radicals and further to form H_2O_2 and $OH^{\bullet}$. A substantial body of evidence has been accumulated indicating that the interfacial electron transfer process involving the reduction of oxygen is the rate-limiting step in the TiO_2-sensitized photodegradation of organics (Turchi and Ollis, 1989). Free radical $HO_2^{\bullet}$ and its conjugate $O_2^{\bullet -}$ are also involved in degradation processes, but these radicals are much less reactive than free hydroxyl radicals.

According to Turchi and Ollis (1989), the hydroxyl radical species reacts strongly with most organic substances by hydrogen abstraction or electrophilic addition to double bonds. Free radicals further react with molecular oxygen to give a peroxyl radical, initiating a sequence of oxidative degradation reactions, which may lead to complete mineralization of the contaminant.

The term mineralization refers to the process by which an organic substrate is converted into CO_2, H_2O and other inorganic ions. Photomineralization refers to the process by which an organic substrate is photodegraded into CO_2, H_2O and inorganic ions upon absorption of light quanta by the photocatalyst or by the adsorbate (Serpone and Emeline, 2002).

1.3.2 Effect of various factors

The influence of some physical parameters governing the kinetics is discussed below. Herrmann (1999) has summarized these effects via plots of rates versus parameters involved as shown in Figure 1.3. This includes mass of catalyst, wavelength of irradiation light, initial concentration of reactant, operating temperature, and radiant flux. The five parameters that govern the kinetics of the photocatalyst behave independently of each other.

1.3.2.1 Mass of catalyst

Either in static or in dynamic flow photoreactors, the initial rates of reaction, *r*, were found to be directly proportional to the mass *m* of catalyst as shown in Figure

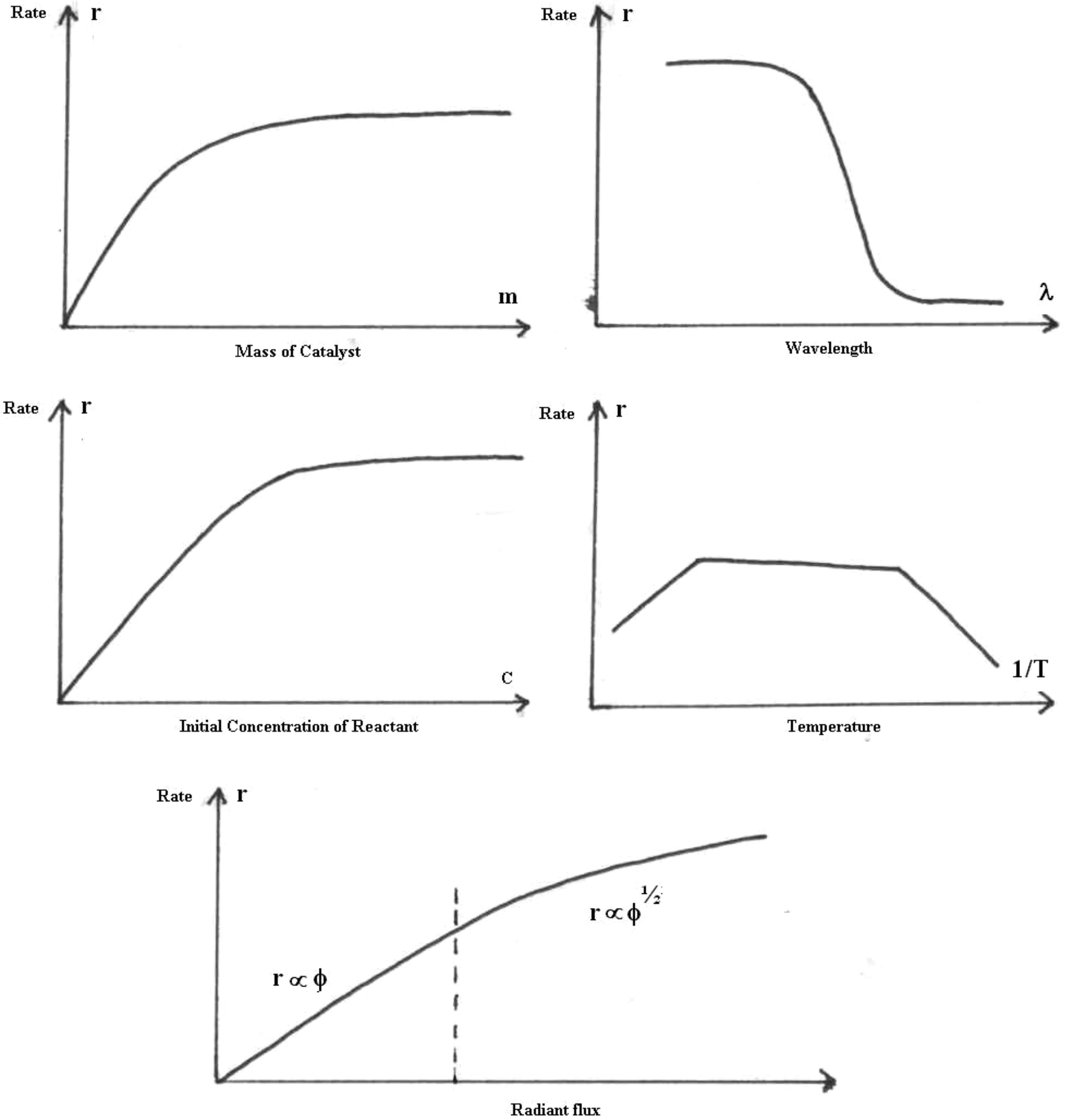

Figure 1.3 Influence of the different physical parameters that govern the reaction rate (generally comprised between 0.1 – 1 mM): (a) mass of catalyst; (b) wavelength; (c) initial concentration of reactant; (d) temperature and (e) radiant flux (Herrmann, 1999).

1.3(a). However, above a certain value of *m*, the reaction rate level was off and becomes independent of *m*. This limit depends on the geometry and on the working conditions of the photoreactor. It was found equal to 1.3 mg TiO_2/cm^2 of a fixed bed and to 2.5 mg TiO_2/cm^3 of suspension. These limits correspond to the maximum amount of TiO_2 in which all the particles – i.e., the entire surface exposed – are totally illuminated. For higher quantities of catalyst, a screening effect of excess particles occurs, which masks part of the photosensitive surface (Herrmann, 1995; 1999).

1.3.2.2 Wavelength

The variations of the reaction rate as a function of the wavelength follows the absorption spectrum of the catalyst as in Figure 1.3(b), with a threshold corresponding to its band gap energy. For TiO_2 having $E_G = 3.02$ eV, this requires: $\lambda \leq 400$ nm, i.e., near-UV wavelength. In addition, it must be checked that the reactants do not absorb the light to conserve the exclusive photoactivation of the catalyst for a true heterogeneous catalytic regime (*no homogeneous nor photochemistry in the adsorbed phase*) (Herrmann, 1995; 1999).

1.3.2.3 Initial concentration

Generally, the kinetics follows a Langmuir–Hinshelwood mechanism confirming the heterogeneous catalytic character of the system with the substrate S and the rate, Γ varying proportionally with the coverage, θ as:

$$\Gamma = k\theta = k(\mathrm{S})\frac{K(\mathrm{S})[\mathrm{S}]_\mathrm{i}}{(1 + K(\mathrm{S})[\mathrm{S}]_\mathrm{i}} \qquad (1.16)$$

For diluted solutions ([S] < 10^{-3} M), K(S)[S] becomes << 1 and the reaction is of the apparent first order, whereas for concentrations > 5 X 10^{-3} M, (K(S)[S] >> 1), the reaction rate is maximum and of the zero order as shown in Figure 1.3(c) (Herrmann, 1995; 1995).

Plots of normalized concentrations vs. irradiation time for phenol at different initial concentrations (40 - 800 μM) were reported by Serpone *et al.* (1996) and the reaction shown can be fitted to a simple rate expression for saturation-type kinetics:

$$\Gamma = k_{\mathrm{obs}} \frac{K_{\mathrm{ads}}[\mathrm{PhOH}]_{\mathrm{i}}}{1 + K_{\mathrm{ads}}[\mathrm{PhOH}]_{\mathrm{i}}} \tag{1.17}$$

Where k_{obs} is the observed rate constant and K_{ads} is the adsorption coefficient of the phenol on the surface of photocatalyst. The K_{ads} value for phenol in 2 g / L suspension at pH 3.0 was found to be $7 \pm 2 \times 10^{3}$ M^{-1}.

1.3.2.4 Temperature

The photonic activation of TiO_2 photocatalysis is usually found to be not particularly temperature sensitive. Thus, the photocatalytic systems do not require heating and are operating at room temperature. The true activation energy E_t is nil, whereas the apparent activation energy E_a is often very small (a few kJ/mol) in the medium temperature range (20 °C ≤ θ≤ 80 °C). However, at very low temperatures (-40 °C ≤ θ≤ 0 °C), the activity decreases and the apparent activation energy E_a increases as shown in Figure 1.3(d). The rate limiting step becomes the desorption of the final product and E_a tends to the heat of adsorption of the product (Herrmann, 1995; 1999). Increasing the temperature should have the effect of lowering the adsorption isotherms associated with the substrate and O_2, and lowering oxygen concentration, $[O_2]$ (Mills and Hunte, 1997).

On the opposite, when θ °C increases above 80 °C and tends to the boiling point of water, the exothermic adsorption of reactant A becomes disfavored and tends to become the rate limiting-step. Correspondingly, the activity decreases and the apparent activation energy becomes negative tending to Q_A (Figure 1.3(d)).

Serpone *et al.* (1996) and Okamoto *et al.* (1985) studied the thermodynamic of photodegradation of 20 mg / L phenol solution, for the range of 12 – 67.5 °C in suspended 2 g / L TiO_2 at pH 3.0. They reported the enthalpy $\Delta H^{\neq}$ of 9.4 ± 0.5 kJ / mol, entropy $\Delta S^{\neq}$ (~ -61 eu) and activation energy E_a (~ 7 - 10 kJ / mol by plotting ln (k / T) vs. 1 / T). The entropy of activation for the oxidative degradation of phenol was large and negative. The rate was seemed to decrease at highest temperature examined.

1.3.2.5 Radiant flux

The rate of reaction r is proportional to the radiant flux Φ as shown in Figure 1.3(e). This confirms the photo-induced nature of the activation of the catalytic process, with the participation of photo-induced electrical charges (electrons and holes) to the reaction mechanism. However, above a certain value, estimated to be approximately 25 mW/cm^2 in laboratory experiments, the reaction rate r becomes proportional to $\Phi^{1/2}$. The optimal light power utilization corresponds to the domain where r is proportional to Φ (Herrmann, 1995; 1995; Serpone *et al.*, 1996; Okamoto *et al.*, 1985).

Photocatalytic process economics are centrally tied to the efficient use of photons. Cost in return is dominated by the efficiency with which solar or lamp photons are harvested for productive light, and subsequent dark, reactions. Photons efficiency can be improved by involving (1) process integration, (2) feedstream conditioning (Gratson *et al.*, 1995), (3) periodic illumination/operation (Szechowski and Noble, 1993; Szcechowski *et al.*, 1993) and (4) reaction integration (Bolton, 1994). These provide a set of high opportunity paths to commercial process development. Seeking photocatalyst efficiency should also involved (1) catalyst deactivation (and regeneration) and (2) catalyst selectivity for desired versus undesired intermediates and final products.

Continued attention is being paid to detecting and identifying intermediates and by-products that can be formed during the photocatalytic process. This is an important tool in developing an understanding of the chemical mechanisms of the processes and is necessary to ensure that potentially harmful substances are not left in the processed stream. As systems are deployed in the field, it is increasingly important that the issues of catalyst lifetime and regeneration be addressed. Related to this is the need to identify those components of water stream that can inhibit or kill catalyst activity. All these are important to the design of efficient and economical treatment systems.

1.3.3 Preparation and modification

TiO_2 coating can be prepared by a range of techniques. These include sol-gel (Cui *et al.*, 2000; Ding *et al.*, 1999; Jiang *et al.*, 1999; Anderson and Bard, 1997; Brezová *et al.*, 1997; Grabner *et al.*, 1991; Dorion *et al.*, 1995; Mikula *et al.*, 1995; Wei and Yan, 1995; Pelizzetti *et al.*, 1993), spray pyrolysis (Chan *et al.*, 1999; Byrne *et al.*, 1998), controlled hydrolysis of $TiCl_4$ or $Ti(OR)_4$ (Cao *et al.*, 1999; Chan *et al.*, 1999; Guo *et al.*, 1998; Wu *et al.*, 1998), plasma enhanced chemical vapor deposition (Cao *et al.*, 1998; 1999; 2000), flame synthesis (Fotou and Pratsinis, 1996; Fotou *et al.*, 1994), chemical vapor deposition (Ding *et al.*, 2000; Guo *et al.*, 1999; Lee *et al.*, 1999), impregnation (Cheng *et al.*, 1995) and electrophoretic coating (Byrne *et al.*, 1998; Chen *et al.*, 2000). These methods can also be utilized to immobilize TiO_2 onto the support substrates.

Some approaches have been focused toward modifying titanium dioxide to increase process efficiency and to improve the overlap of the absorption spectrum of the TiO_2 with the solar spectrum. These can be done by metallized titanium dioxide with noble metals (Pt (Brezová *et al.*, 1997), Ag (Cui *et al.*, 2000; Alberici and Jardim, 1994), Pd, Au, Ni, Cu), doping with transition metal ions (Fe (Brezová *et al.*, 1997; Bickley *et al.*, 1993), Cr (Leyva *et al.*, 1998; Brezová *et al.*, 1997; Anpo, 2000), V, Si (Deng *et al.*, 2000; Deng *et al.*, 2000; Anderson and Bard, 1997; Fotou and Pratsinis, 1996)) and conjunction of dye sensitizer with titanium dioxide (Chatterjee and Mahata, 2001). Depositing metals over titanium dioxide is to improve the electron-hole separation and to increase the rate of the reduction process due to the catalytic properties of the metal itself had also been studied (Sclafani *et al.*, 1997).

1.3.4 Inorganics and metal ions remediation

Unlike the organic compounds, only some inorganic compounds can be treated by TiO_2 photocatalyst. For instance, nitrite is oxidized into nitrate, sulphide, sulphite and thiosulphate are converted into sulfate, whereas cyanide is converted into isocyanide, nitrogen and nitrate that are harmless.

Photocatalysis not only has been studied as a mean of the destruction of organic pollutants in solution via photocatalytic oxidation (Ollis and Al-Ekabi, 1993; Hoffmann *et al.*, 1995), but also as a way to photoreduce and recover heavy metals (Prairie *et al.*, 1992). Heavy metals such as Pb^{2+}, Mn^{2+}, Tl^{+}, and Co^{2+} become oxides, while Ag^{+}, Au^{2+}, Pd^{2+}, Pt^{2+}, Cu^{2+} and Hg^{2+} are reduced, and settle on the titanium dioxide surface. Since their reduction-oxidation potential is pH dependent, metal ions can be precipitated out, in sequence, by photocatalytic reaction under different pH (Tanaka *et al.*, 1996; Herrmann, 1999). These metals could be subsequently recovered by dissolution in acid that regenerated the original titanium dioxide particles (Serpone and Pelizzetti, 1989).

1.3.5 Activity evaluation

It is well known that the efficiencies of TiO_2 vary substantially by their type, synthesizing method, preparation method (Sclafani *et al.*, 1990), and the target pollutants (Serpone *et al.*, 1996). This situation makes it hard to compare the performance of different photocatalysts. Proposed methods of evaluating photocatalyst activity include: (1) the speed of organic decomposition, (2) probing with a chemical illuminant or fluorescent substance, (3) ESR (electron spin resonance) measurement, (4) speed of dyestuff decomposition of methylene blue, (5) amount of removed NO_x and (6) amount of hydrogen and oxygen generated in water decomposition (Sclafani *et al.*, 1990).

It has been demonstrated that various parameters have effects on the degradation rate of compounds (Al-Sayyed *et al.*, 1991; D'Oliveira *et al.*, 1990). A few degradation kinetic expressions of different compounds have been reported in the literature. Unfortunately, some of these studies investigated the effects of various parameters on the initial degradation rate, such as the initial disappearance rate of organic compounds (Inel and Okte, 1996) or the initial formation rate of CO_2 (Matthews, 1988; Mills and Morris, 1993), rather than the degradation rate during the whole photodegradation or photomineralization process. Meanwhile, initial rate data are tedious to obtain and subject to variation. This will reduce the reliability of the results. In this project, most of the rate expressions are based on the whole disappearance of the target pollutant. The determining step in the photocatalytic activity of the TiO_2 has not been considered in the design of the experiments.

1.3.5.1 Kinetic

As mentioned earlier, the kinetics of heterogeneous photomineralization of organic substrates by oxygen, sensitized by TiO_2, on steady state illumination fit a Langmuir-Hinshelwood kinetic scheme, that is the relationship between the initial pollutant concentration and the initial rate of removal followed Langmuir form.

$$\Gamma_{\mathrm{i}} = -\frac{\mathrm{d}[\mathrm{S}]_{\mathrm{i}}}{\mathrm{d}t} = k_{\mathrm{s}} \frac{K_{\mathrm{s}}[\mathrm{S}]_{\mathrm{i}}}{1 + K_{\mathrm{s}}[\mathrm{S}]_{\mathrm{i}}} \qquad (1.18)$$

where Γ_i is the initial rate of substrate removal, $[S]_i$ is the initial concentration of the organic substrate and, traditionally, K_s is taken to be the Langmuir adsorption constant of species S on the surface of TiO_2 and k_s is a proportionality constant which provides a measure of the intrinsic reactivity of the photoactivated surface with S.

The equation can be simplified to an apparent first-order equation:

$$\ln\frac{[S]_i}{[S]} = k_s K_s t = k't \tag{1.19}$$

thus, a plot of $\ln\frac{[S]_i}{[S]}$ vs. time represents a straight line, the slope of which upon linear regression equals the apparent first-order rate constant *k'* (Wang *et al.*, 1999; Serpone *et al.*, 1996). Furthermore, plots of reciprocal initial rate vs. reciprocal initial substrate concentration [Γ_i–1 vs. $[S]_i$–1] will produced the necessary linear plots for organic substrates (Turchi and Ollis, 1990).

Generally, the value of K_s derived from a kinetic study is not directly equivalent to the dark adsorption isotherm for S on the semiconductor; the latter values are usually much smaller. It is found that k_s is proportional to I^{θ}_a, where I_a is the rate of light absorption and θ is a power term which is equal to 0.5 or unity at high or low light intensity respectively. It is also found that k_s is proportional to the fraction of O_2 adsorbed on TiO_2, where $f(O_2)$ is given as

$$f(O_2) = \frac{K_{O_2}[O_2]}{1+K_{O_2}[O_2]} \tag{1.20}$$

K_{O2} is the Langmuir adsorption coefficient for O_2 on the TiO_2 (Mills and Hunte, 1997).

Okamoto *et al.* (1985) studied the photocatalytic decomposition of phenol over anatase TiO_2 powder. They found this photocatalytic degradation followed the first-order kinetics, up to high conversions, of which the apparent rate constant k_{ap} depended on initial concentration of phenol $[\text{phenol}]_0$, $[TiO_2]$, O_2 pressure p_{O2}, and incident light intensity I. The results were satisfactorily explained by the equation;

$$\Gamma = \varphi_{\mathrm{OH}\bullet} I_{\mathrm{a}}^{\mathrm{n}} \frac{K_{\mathrm{O_2}} p_{\mathrm{O_2}}}{1 + K_{\mathrm{O_2}} p_{\mathrm{O_2}}} \frac{[\text{phenol}]}{[\text{phenol}]_{\mathrm{i}} + \beta'} \tag{1.21}$$

where Γ is the reaction rate; $\varphi_{\bullet\mathrm{OH}} I_{\mathrm{a}}^{\mathrm{n}}$, a parameter related to the formation rate of $OH^\bullet$ radicals or real reactive species; K_{O2} the equilibrium constant of Langmuir adsorption of O_2; β', the ratio of the combined first-order rate constant of the reaction of $OH^\bullet$ with species other than organic compounds to the second-order rate constant of the reaction of $OH^\bullet$ with phenol (Robert *et al.*, 2000).

1.3.6 Immobilized photocatalysts

Photocatalytic treatment of water pollutants can be accomplished either by using suspension or immobilized TiO_2. Most works have utilized TiO_2 in suspension mode because of its high photoactivity due to its higher available surface area and superior mass transfer properties (Trillas *et al.*, 1996). Utilization of TiO_2 in immobilized mode is more practical because it solves the problems of separation, recovery and reuse as compared to suspension mode (Brezová *et al.*, 1997; Peill and Hoffmann, 1995; Matthews, 1988). Most immobilization has been prepared on glass (Cui *et al.*, 2000; Dumitriu *et al.*, 2000; Fan *et al.*, 1999; Jiang *et al.*, 1999; Kumara *et al.*, 1999; Blazkova *et al.*, 1998; Brezová *et al.*, 1997; Preis *et al.*, 1996; Preis *et al.*, 1997; Trillas *et al.*, 1996; Brezová *et al.*, 1995; Mikula *et al.*, 1995), organic polymer

(Tennakone *et al.*, 1995), silica gel (Ding *et al.*, 2000; Zheng *et al.*, 2000; Alemany *et al.*, 1997;1998), zeolite, thin films (Guo *et al.*, 1999; Wu *et al.*, 1998), metal (Byrne *et al.*, 1998) and carbon (Matos *et al.*, 1998).

In general, TiO_2 immobilization can be carried out either by *in situ* catalyst generation (precursor usually titanium alkoxide) or by manipulation of previously made TiO_2 powder (PMTP) (Pozzo *et al.*, 1999). Immobilization via precursors (for examples sol-gel, spin coating, spray pyrolysis and chemical vapor deposition) have several limitation compared to PMTP such as involvement of toxic alkoxides precursors, long preparation time and/or special equipments.

The development of an electrophoretic method for the direct immobilization of powder TiO_2 on conducting support substrates is an important step for the development of industrial scale photocatalytic reactors. The method allows commercially available TiO_2 with high photocatalytic activity (such as Degussa P25) to be applied to comparatively inexpensive support substrates such as aluminium, stainless steel and even conducting plastics. In addition, the product reserves many favorable powder characteristics relative to those derived from conventional precursor routes.

The thickness can be controlled either by the voltage applied and/or the time for which the voltage is applied and the technique allows for thick films to be prepared in a matter of seconds. In contrast, Bockelmann *et al.* (1994) reported that 10 coating were required using a dip coating method to build up catalyst coverage of 1 mg / cm^2. The equipment required for electrophoretic deposition is cheap compared to high vacuum or spray pyrolysis techniques. None of the expensive and toxic alkoxides commonly employed in the precursor methods are required. Thermal treatment as in all precursor methods is eliminated and the products are readily used. Furthermore, coated supports on which the catalyst has become inactive could easily be cleaned and recoated with new catalyst. Electrophoretic deposition lends itself to the processing of awkwardly shaped substrates and therefore innovative reactor design. The electrophoretic coating method was found to be the most reproducible coating process resulting in highly fractured thick films with high photocatalytic activity (Byrne *et al.*, 1998). Electrophoretic method however suffers from poor coating adhesiveness whereby coated TiO_2 leaches out easily. Therefore, good TiO_2 adhesion to the support is important. The coating should resist strain derived from particle-fluid mechanical interactions in the environment, in order to avoid detachment of TiO_2 particles from the support. Unfortunately, good strength of coating and photoactivity appear to be usually in an inversion relation (Pozzo *et al.*, 1997). Therefore, a careful examination of the TiO_2/support interaction especially with regard to the adherence of the former is needed to optimize the photocatalytic activity of the TiO_2. A systematic comparison between suspended and immobilized photocatalysts when the latter activity is taken before and after immobilization is needed to test the achievement of the immobilization procedure (Bideau *et al.*, 1995).

The adsorption characteristics are important in the removal of low concentration of pollutants (Matthews, 1988; Torimoto *et al.*, 1996). Since the oxidation reaction occur at the surface of the TiO_2, the attachment of TiO_2 to an adsorbent support will provide several benefits such as increasing the surface contact time (if a substrate that is strong adsorbent for molecule weakly adsorbed by TiO_2 is selected, thus increase the rate of mineralization), preventing the release of the intermediates (in some cases may be more harmful than the target pollutant) (Okamoto *et al.*, 1985) and the adsorbent may continuously regenerated *in situ* by the TiO_2 oxidation of adsorbed pollutants (Matthews, 1988).

Previous electrophoretic immobilization of TiO_2 powder on stainless steel was reported by Fernandez *et al.* (1995). In the report, the TiO_2 immobilized on stainless steel compared poorly with TiO_2 immobilized onto quartz by dip coating of a sol precursor. The decline in activity has been correlated with the presence of cationic impurities (Si^{4+}, Na^{+}, Cr^{3+}, Fe^{3+}) in the layer as a consequence of the thermal treatments to improve the cohesion of the TiO_2 layer and it adhesion onto the support. However, they annealed the coated stainless steel at 973 K that led to deactivation of the catalyst. Byrne *et al.* (1998) reported lower annealing temperatures to give adequate adhesion and the electrophoretic coating of TiO_2/stainless steel (573 K), TiO_2/Ti (573 K), TiO_2/Ti alloy (773 K) and TiO_2/SnO_2 glass (673 K) whereby reproducible thick films with high photocatalytic activity were obtained. But at annealing temperature below 573 K, significant catalyst stripping occurred and at higher voltage (> 25 V), the film deposition was hard to control due to the short time intervals involved. Also, deposition at lower voltages gave thinner films and highly porous fractured appearance due to thermal expansion.

Several problems of immobilizing metal oxide powders with electrophoretic method were found by previous researchers. In general, the strength of deposit and the sustainability of catalyst activity by this method were low. The surface of support substrate was not totally covered by the deposit especially at low potential employed.

The aggregation of deposit was not homogeneous, not smooth and tends to be fractured (Byrne *et al.*, 1998). The strength and adhesion of immobilized metal oxide particles was not high, consequently, this leads to the detachment of particles from the support (Pozzo *et al.*, 1997; Bideau *et al.*, 1995). Therefore, thermal treatment at high temperature was always employed to improve the adhesion of particles to the support. In addition, the high temperature would lead to activity decline due to the formation of impurities (such as Si^{4+}, Na^{+}, Cr^{3+}, Fe^{3+} from stainless steel at 973 K) in the layer and also due to conversion of some TiO_2 anatase form to rutile (Fernandez *et al.*, 1995).

In this research, conducting materials such as metal and conducting plastic plates have been chosen as support substrates because they are readily available, relatively inexpensive, can be modified easily and can be fabricated into any shape, and have high mechanical strength.

1.4 Treatment of Phenol

Contamination of water resources by a variety of organic substances is an increasingly common problem. Phenols represent an important class of environmental water pollutant. These organic compounds have been considered on the EPA's priority pollutants list since 1976. Most phenolic compounds are present in waste water from petrochemical, coal tar, plastic and pesticide chemical industries, which produce them as chemical intermediates or generate them during treatment of effluents containing phenolic compounds (Hoffmann *et al.*, 1995; Soria *et al.*, 1993; Schiavello, 1988; Serpone and Pelizzetti, 1989; Auguglizro *et al.*, 1988; Sclafani *et al.*, 1990). Phenol is a refractory and common compound in industrial waste. The fate of these compounds is of interest because of their toxicity to humans and to aquatic life. The destruction of these pollutants is therefore a priority. The parent molecule, investigated in this work, is also a good model of the fate of the aromatic ring in environmental photodegradations.

The mechanistic aspects of the phenol photodegradation when TiO_2 is used as catalyst had already been reported in the literature (Okamoto *et al.*, 1985; 1995; Ollis and Al-Ekabi, 1993). Okamoto *et al.* (1985) studied the photocatalytic decomposition of phenol in oxygenated aqueous suspensions of lightly reduced anatase TiO_2, and the results indicated that phenol was completely mineralized to CO_2 in the presence of TiO_2 powder under solar irradiation without both aeration and mixing of the solution.

1.4.1 Mechanistic studies

Two general mechanisms for photomineralizations of phenol to CO_2 and H_2O are currently being debated: (i) the photogenerated holes oxidize adsorbed phenol (D_{ads}) directly according to

$$D_{ads} + h^+_{VB} \rightarrow D^+_{ads} \qquad (1.22)$$

Or (ii) they first oxidize adsorbed water or OH^- groups to give the $\equiv Ti\text{-}^{\bullet}OH$ radical:

$$\equiv Ti - OH^-_{surf}\,(\text{or } H_2O) + h^+_{VB} \rightarrow \equiv Ti - OH^{\bullet}_{surf}\ (\text{and } H^+) \qquad (1.23)$$

In turn, the hydroxyl radical oxidizes adsorbed phenol to yield hydroxylated radical intermediates, e.g. hydroquinone, pyrocatechol and others (Okamoto *et al.*, 1985). Subsequently, these react further to yield the final products CO_2 and H_2O. Note that the intermediates evoked in mechanism (ii) may also result from mechanism (i) if oxidized phenol (a cation) reacted with water (Fox *et al.*, 1991; Stafford *et al.*, 1997; Serpone *et al.*, 1993).

Okamoto *et al.* (1985) have reported on the reaction pathway of the photocatalytic decomposition of phenol in oxygenated aqueous suspensions of anatase TiO_2 (Figure 1.4). According to them, hydroxyl radicals are real reactive species responsible for the reaction. They were formed not only by the reaction of holes with adsorbed H_2O or OH^-, but also via H_2O_2 from $O_2^{\bullet -}$ formed by electron trapping of adsorbed O_2. Phenol was decomposed initially via its hydroxylated compounds into pyrocatechol, hydroquinone and/or benzoquinone. These intermediates were further degraded into pyrogallol, hydroxyhydroquinone and/or hydroxybenzaquinone before opening up the C_6 ring into the final products of CO_2 and H_2O (refer to Figure 1.4). The products identified in the photo-oxidation of phenol may originate either by $OH^\bullet$ radical attack of the phenol ring, or by direct hole oxidation to give the cation radical that subsequently undergoes hydration in solvent water (Pelizzetti and Minero, 1993). It is interesting from the viewpoint of wastewater treatment that phenol is completely mineralized to CO_2 in the presence of TiO_2 powder under solar irradiation without both aeration and mixing of the solution. The optimum pH was found to be 3.5 (Okamoto *et al.*, 1985).

Serpone *et al.* (1996) and Tahiri *et al.* (1996) identified two hydroxylated phenyl intermediates, which are hydroquinone (1,4-dihydroxybenzene) and catechol or pyrocatechol (1,2-dihydroxybenzene) in nearly equal amounts, in using Hombikat UV-100 TiO_2 and Sargent-Welch TiO_2 in suspension at pH 3. However, only hydroquinone was observed as hydroxylated aromatic intermediate when Degussa

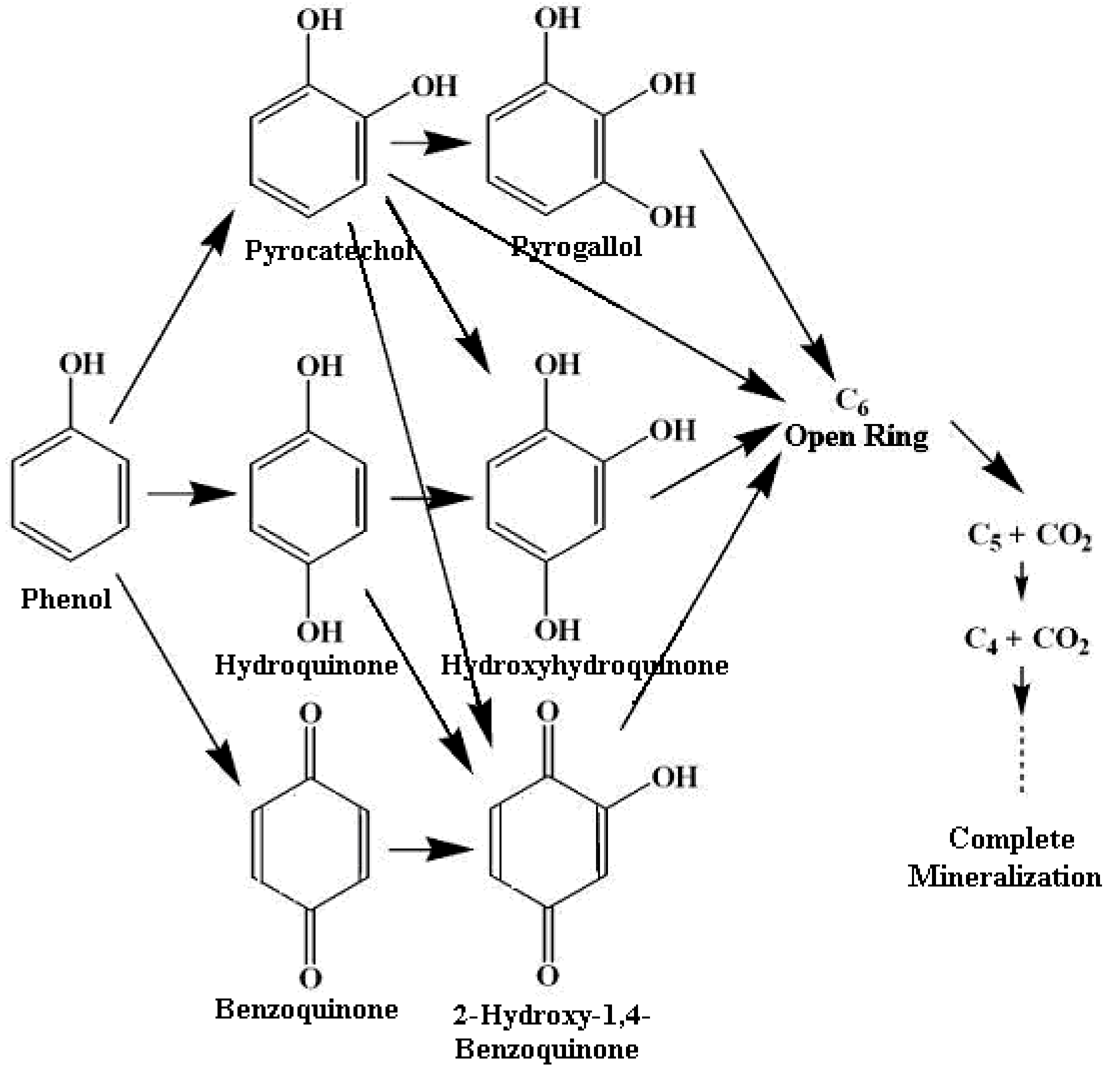
OH
OH
OH
OH
OH
Pyrocatechol
Pyrogallol
OH
OH
OH
OH
C6
Open Ring
C5 + CO2
C4 + CO2
Phenol
OH
OH
Hydroquinone
Hydroxyhydroquinone
O
O
OH
O
O
Complete Mineralization
Benzoquinone
2-Hydroxy-1,4-Benzoquinone

Figure 1.4 Proposed mechanism of photocatalytic degradation of phenol (Okamoto *et al.*, 1985).

P25. Phenol disappeared faster in the presence of irradiated Sargent-Welch TiO_2 than in an illumination Degussa P25 TiO_2 suspension (Serpone *et al.*, 1996). In all cases, phenol disappears via apparent first-order kinetics.

Pyrocatechol and hydroquinone have been detected as hydroxylated products in the studies of photocatalytic oxidation of phenol on TiO_2 by Wang *et al.* These intermediates degraded rapidly via fumaric acid, organic acids and finally to CO_2 (Hu *et al.*, 2000).

Sclafani *et al.* (1998) reported hydroquinone, catechol and muconic acid were the main intermediates for the phenol photodegradation in aqueous Degussa P25 TiO_2 suspension. However, in another experiment that employed Merck TiO_2, quinone was also detected.

Although photodecomposition of phenol in aerated aqueous TiO_2 suspensions leads finally to CO_2 and H_2O, a number of aromatic (Okamoto *et al.*, 1985) and aliphatic (Pichat *et al.*, 1993) intermediates wee also obtained. Recent investigations have shown a big difference between phenol and TOC diminution (Sobezynski *et al.*, 1997), confirming thus the existence of a number of reaction intermediates. Most recent studies on photocatalytic oxidation of phenol on illuminated TiO_2 show that several ring intermediates like di- and trihydroxybenzenes are present in the reaction mixture. It has also been observed that hydroquinone and p-benzoquinone are the major intermediates of the process (Sobezynski *et al.*, 1999).

In conclusion, phenol photocatalytic oxidation in water by TiO_2 has different reaction pathways and intermediates, depending on the source of TiO_2 used, support substrates and experimental conditions (Bickley *et al.*, 1993).

1.4.2 pH

Hoffmann *et al.* (995) reported that the point of zero charge (pzc) for TiO_2 is at pH ~ 6.25. This implies that the interactions with cationic electron donors and electron acceptors will be favored for heterogeneous photocatalytic activity at high pH under conditions in which the $pH > pH_{pzc}$, while anionic electron donors and acceptors will be favored at low pH under conditions in which $pH < pH_{pzc}$.

The pH of an aqueous solution significantly affects all oxide semiconductors, including the surface charge on the semiconductor particles, the size of the aggregates formed and the energies of the conductance and valence bands. Despite this, the rate of reaction sensitized by TiO_2 is not usually found to be strongly pH dependent. Typically Γ_i varies by less than one order of magnitude from pH 2 to pH 12. Higher reaction rates for various TiO_2-sensitized photomineralizations have been reported at both low and high pH (Hoffmann *et al.*, 1995). Generally, it is found that perchlorate and nitrate anions have little effect on kinetics of reaction, whereas sulphate, chloride and phosphate ions, especially at concentrations of greater than 10^{-3} mol/L, can reduce the rate by 20 - 70% due to the competitive adsorption at the photoactivated reaction sites.

The amount of phenol adsorbed by TiO_2 particles increased markedly with decreasing solution pH. Thus, higher removal of phenol by photocatalysis is always obtained in acidic solution. This is because in neutral and acidic solutions, the undissociated species (C_6H_5OH) is the predominant species and has a higher affinity for TiO_2 particles as compared to phenolate anion ($C_6H_5O^-$), which is predominant in alkaline solution (Ku *et al.*, 1996).

The surface is positively charged at pH below pH_{pzc} and negatively charged above pH_{pzc} about 6 (Terzian, 1993; Terzian and Serpone, 1995). The pKa of phenol is pH ~ 10 and at higher pH values there is considerable amount of negatively charged phenoxide species. Therefore in alkaline solutions pH > 10 an electrostatic repulsion between the two negatively charged species phenoxide and TiO_2 is expected (O'Shea and Cardona, 1995). In most cases, photo-oxidation was carried out at pH 3, in order to minimize direct photolysis known to occur significantly in alkaline media.

In acidic media (pH 3), the superoxide radical anion protonates to give the hydroperoxide radical, $HO_2^\bullet$ (pKa 4.88). Other reactions that no doubt occur on the TiO_2 particle surface and that are solvent (water) related are summarized in equations below (Pelizzetti and Minero, 1993).

$$O_{2(ads)}^{\bullet-} + H^+ \rightarrow HO_{2(ads)}^{\bullet} \tag{1.24}$$

$$2\,HO_2^\bullet \rightarrow H_2O_2 + O_2 \tag{1.25}$$

$$O_2^{\bullet-} + HO_2^\bullet \rightarrow O_2 + HO_2^- \xrightarrow{+H^+} H_2O_2 \tag{1.26}$$

$$H_2O_2 + e^- \rightarrow OH^\bullet + OH^- \tag{1.27}$$

$$H_2O_2 + OH^\bullet \rightarrow H_2O + HO_2^\bullet \tag{1.28}$$

1.4.3 Inorganic ions

In the presence of metal ions M^{n+} the photogenerated electrons and holes may be involved in the surface reduction and oxidation processes. The presence of Ca^{2+}, Mg^{2+}, $Zn^{2+}$and Ni^{2+} in the concentration range of 0.28 – 1.1 mM had no influence on the phenol degradation rate (Brezová *et al.*, 1995).

Theoretically, the presence of iron salts, e.g., $FeCl_3$ promote the degradation of phenol. By the reduction of Fe^{3+} ions, the dissolved Fe^{2+} are formed, which can additionally produce $OH^{\bullet}$ radicals via the photo-Fenton reaction with H_2O_2 generated in photocatalytic system. So, in the irradiation of aqueous TiO_2 suspension in the presence of Fe^{3+} ions, two sources of hydroxyl radical generation are present (Shul'pin *et al.*, 1997; Brezová *et al.*, 1995). However, Wei *et al.* (1990), Brezová *et al.* (1995) and Scalfani and Palmisano (1991) found 'promotion-inhibition' type kinetic in the presence of Fe^{3+}. The optimum degradation rate was obtained at pH 2.0 with $[Fe^{3+}] = 4.8$ mM, pH 3.0 with $[Fe^{3+}] = 0.6$ mM and pH 3 with $[Fe^{3+}] = 0.5$ mM respectively.

Brezová *et al.* (1995) reported that the dissolved Cu^{2+} ions inhibited phenol degradation. Cupric ions were reduced to Cu^0 and the deposition of metal copper could be observed on the surface of TiO_2. The deposition of elemental copper could significantly change the surface properties of TiO_2 (separation of charge carriers, adsorption of phenol), and the observed phenol degradation rate was lower (Brezová *et al.*, 1995). However, Okamoto *et al.* and Butler and Davis (1993) found 'promotion-inhibition' type kinetic in the presence of Cu^{2+} at pH 3.5 with decreased rates at higher concentrations and pH value. The optimum degradation rate was obtained when [Cu^{2+}] was 10^{-4} M. On the other hand, inhibition type kinetic at pH 4.0 was found by Wei *et al.* (1990).

The addition of 0.28 mM Cr^{3+} in the TiO_2 suspension resulted in the strong decrease of phenol degradation rate in TiO_2 suspension. The detrimental effect of Cr^{3+} was explained by the fact that trivalent ion is believed to create acceptor and donor surface centers that behave as recombination centers of the photoproduced charge carriers. Similarly, ion doping using Al^{3+} was also found to strongly inhibit the reaction, because of trivalent acceptor impurities behave as electron-hole recombination centers. For ion doping, either of the *p*-type obtained by dissolving in the lattice of TiO_2 heterocations of valency lower than that of Ti^{4+} (Al^{3+}, Cr^{3+}, Ga^{3+}) or of the *n*-type obtained by dissolving heterocations of valency higher than +4 (Nb^{5+}, Ta^{5+}, Sb^{5+}) the inhibiting effect was ascribed to an increase in the electron-hole recombination rate. Actually, *p*-type doping agent creates acceptor centers which trap photo-electrons and then, once negatively charged, attract holes, thus behaving as recombination centers (Brezová *et al.*, 1995; Shul'pin *et al.*, 1997).

An increase was observed in the catalytic activity of the TiO_2 when loaded with silver, as previously described by Cui *et al.* (2000), Herrmann *et al.* (1997) and Alberici and Jardim (1994). The apparent increase observed in activity is principally due to the increase in the exposed surface due to the textural characteristics of the Ag-TiO_2 layer in comparison with TiO_2. The Ag-TiO_2 layer appeared to have a smoother surface compared to TiO_2 layer that is morphologically granular. This meant that the Ag-TiO_2 coatings contained smaller grains compared to pure TiO_2, which correspondingly gave a higher exposed surface. Another cause as pointed out by Hermann *et al.* (1997), the presence of metallic silver always produced an increase in activity because of the increase in the electron-hole pair separation efficiency (preventing the electron-hole recombination) induced by trapping of electrons by metallic silver.

The influence of chloride ions on photocatalytic degradation of phenol varies with pH. At pH 3, the chloride ion (NaCl) showed significant inhibition, but not so much at pH 7 and 11. At pH 3, $TiOH^{2+}$ and TiOH were the main functional groups on the catalyst surface, and the chloride ions competed with organic species for active sites and lowered the reaction rate. For higher pH, the negatively charge catalyst surface repulsed the approach of chloride ions to the surface and retarded their adsorption, but without influence on the decomposition of organics. Another cause as pointed out in the literature (Auguliaro *et al.*, 1991), chloride ions competed with oxygen for electrons, therefore, reduced the formation of $O_2^{\bullet -}$ radicals and then blocked the chain reaction for hydroxyl free radicals as proposed by Okamoto *et al.* (1985). The third reason was given by Wang *et al.* (1999) and it was related to the combination of chloride ions with free radicals during reaction, therefore, decreased the reactive chances between reactant and free radicals, and slowed down the decomposition.

1.4.4 Added oxidant

Oxygen is the most common oxidant for photocatalytic reactions, but other oxidants, such as hydrogen peroxide (Prousek and Velic, 1996; Augugliaro *et al.*,

1995) have been found to improve reaction rates with a variety of organic substrates under certain conditions. A photocatalytic reaction in the presence of H_2O_2 usually shows some advantages due to an increase in the concentration of $OH^{\bullet}$ via H_2O_2 following the mechanism given by Wei *et al.* (1990):

$$H_2O_2 + O_2 \rightarrow OH^{\bullet} + O_2 + OH^{-} \qquad (1.29)$$

$$H_2O_2 + h\upsilon \rightarrow 2OH^{\bullet} \qquad (1.30)$$

$$H_2O_2 + e^{-}(TiO_2) \rightarrow OH^{\bullet} + OH^{-} \qquad (1.31)$$

This indicates the electron scavenging capability of H_2O_2, thereby preventing the recombination between photogenerated electrons and holes. Therefore, hydrogen peroxide acts both as an additional e- scavenger (Eq. 1.32) in addition to O_2 and as an oxidizing agent (Eq. 1.33) (Hofstadler *et al.*, 1994)

$$TiO_2(e^{-}) + H_2O_{2,ads} \rightarrow OH^{-}_{ads} + OH^{\bullet}_{ads} \qquad (1.32)$$

$$H_2O_{2,ads} + OH^{\bullet}_{ads} \rightarrow H_2O_{ads} + HO^{\bullet}_{2,ads} \qquad (1.33)$$

H_2O_2 is considered to have two functions in the process of photocatalytic degradation. It accepts an electron and thus promotes the charge separation and also forms $OH^{\bullet}$ which is a strong oxidizing agent (Legrini *et al.*, 1993). The enhanced reaction rates by hydrogen peroxide presumably is increasing the slow step for trapped electron removal, thus diminishing electron-hole recombination and increasing the selective consumption of holes for surface oxidations. In the presence of excess H_2O_2, however, TiO_2 reacts with H_2O_2 to form peroxo compounds such as $Ti(O)_2(OH)_2$ and $Ti(OOH)(OH)_3$ which are detrimental to the photocatalytic action. This explains the need of an optimum concentration of the H_2O_2 for the maximum effect (Rivera *et al.*, 1993).

1.5 Statement of Problems

The immobilization of TiO_2 powder with electrophoretic method suffers from several problems:

a. production of non-smooth and fractured TiO_2 layer
b. poor coating adhesiveness whereby coated TiO_2 leaches out easily
c. low sustainability of photocatalytic activity

1.6 The Research Objectives

The main aim of this research is to exploit the well-established photocatalytic characteristics of TiO_2 in a more practical and sustainable ways. This work describes the development of direct anatase TiO_2 powder immobilization method and studies of its effectiveness. Studies were focused on the effect of various supporting substrates in immobilized photocatalysts since supports markedly influence the inherent properties of the photocatalyst. Al, Cu, Cu/Ni bimetal, PET/Ag and PET/C had been chosen as supports while phenol in aqueous solution was used as the model pollutant. Aluminium plate was chosen due to its relatively cheap cost and easily available. Copper, PET/silver plates were used because of positive photocatalytic effect of copper and silver. PET/carbon was used because of high adsorption of carbon. Copper/nickel bimetal was used as nickel was known as catalyst and not much works have been done involving bimetal support.

All immobilized photocatalysts were prepared via electrophoretic method (Fernandez *et al.*, 1995). The photocatalytic activity of Al/TiO_2, $Al/ENRTiO_2$, Cu/ENRTiO_2, Cu/Ni/ENRTiO_2, PET/Ag/ENRTiO_2 and PET/C/ENRTiO_2 was evaluated by degradation of phenol solution.

The objectives of this research include:

(a) To modify electrophoretic method as an immobilization technique for improving adhesiveness by using epoxidized natural rubber (ENR),

(b) Fabrication of immobilized TiO_2-ENR system on various support substrates,

(c) To optimize the fabrication parameters and solution parameters for photocatalytic degradation of phenol solution,

(d) To evaluate the efficiency and effectiveness of various immobilized TiO_2-ENR systems towards degradation of phenol as compared to conventional electrophoretic deposition, sol-gel and suspension modes,

(e) To assess the effect of supporting materials on the photocatalytic degradation of phenol solution, and

(f) To study the effect of anions and cations on the photocatalytic degradation of phenol solution.